Communication Issues in Decentralized Kalman Filters

Markus S. Schlosser and Kristian Kroschel
Institut für Nachrichtentechnik
Universität Karlsruhe
76128 Karlsruhe, GERMANY
{schlosser, kroschel}@int.uni-karlsruhe.de

Abstract – *Decentralized Kalman Filters are often used in multi-sensor target tracking as such a distributed fusion architecture has several advantages compared with centralized ones. On the other hand, distributed fusion is not only conceptually more complex but the required bandwidth is also likely to be a lot higher. This is especially true if the final estimate shall be obtained at several fusion nodes or if non-linearities are present in the system. However, a trade-off between bandwidth and performance is possible. In this work, the quantitative amount of performance degradation due to a reduction in communication rate between the processing nodes is investigated for a decentralized Kalman filter in typical tracking scenarios. Furthermore, as a conclusion, a simple approach to deal with asynchronous measurements is proposed.*

Keywords: Multi-sensor, target tracking, decentralized Kalman filter (DKF), reduced communication rate, performance degradation, asynchronous measurements

1 Introduction

In target tracking, multi-sensor systems are becoming more and more popular. The advantages especially for physically distributed sensors are obvious: multiple viewing angles, different strong points of different sensors and higher robustness due to the inherent redundancy. On the other hand, some kind of fusion is necessary to integrate the data from the different sensors and to extract the desired information about the targets.

Traditionally, a centralized fusion architecture was used, where all the data from the different sensors was sent to a single location to be fused. In recent years, increasing emphasis has been placed on distributed fusion where several fusion nodes exist in the network, like e.g. the Decentralized Kalman Filter (DKF). The advantages of such a distributed fusion architecture are: higher robustness due to redundancy of fusion nodes and lower processing load at each fusion node. For a large number of sensors, centralized fusion might not even be applicable at all if the central processor cannot handle the large amount of data transmitted by the sensors.

On the other hand, distributed fusion is conceptually a lot more complex. For example, common information has to be detected and discarded in the fusion process. Additionally, the task of data association in tracking multiple targets, which is already difficult and still an active area of research for the centralized fusion architecture, becomes even more complex in the distributed case where only parts of the data are available at each fusion node.

Furthermore, the required bandwidth is also likely to be a lot higher compared with centralized fusion. This is especially true if the final estimate shall be obtained at several fusion nodes. However, a trade-off between bandwidth and performance is possible by letting the fusion nodes communicate at reduced rates. Along this line, it was proposed in [1] to transmit track estimates only if the error of the predicted position exceeds some prespecified tolerance.

Nevertheless, most research on DKFs assumed an unlimited communication bandwidth between the different processing nodes [2, 3]. In [4, 5, 6], it was already pointed out that the information conveyed by the different local processors becomes correlated due to propagating the same underlying process noise if the communication rate is reduced. However, no quantitative measures for the amount of performance degradation were given. This shall be investigated here.

To keep the treatment simple, we focus on communication issues in a simple DKF consisting of two Local Kalman Filters (LKFs) producing track estimates based on a single local Sensor (S) and a Fusion Center (FC) combining these local estimates to a global one, as presented in Fig. 1.

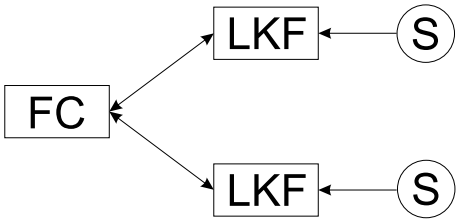

Fig. 1: DKF for two sensors

This scenario is inspired by one of our projects, i.e. a humanoid robot equipped with a microphone array and a stereo-camera tracking a human walking around in an office room. The sensor systems measure the position of the target in spherical coordinates whereas the target dynamics are best described in Cartesian ones. Thus, there is a nonlinear relationship between the measurement vector and the state vector.

As will be discussed later, this requires the Kalman Filters (KFs) at the local processors to receive feedback of the global estimate from the fusion center to achieve the best performance. Therefore, in this work the amount of performance degradation shall also be investigated for reducing the feedback rate in such a tracking scenario.

Sensors running at different observation rates are an important issue in distributed target tracking, too. In [7], a rather complex algorithm was deduced to cope with asynchronous measurements in a DKF requiring feedback from the FC to the LKFs. Based on our findings concerning the reduction in communication rate, a simple alternative to treat asynchronous measurements will be presented here.

2 Decentralized Kalman Filter

For a Kalman Filter (KF) to be applicable, the target's dynamics need to be modeled by the following state space equation

$$\mathbf{x}(k+1) = \mathbf{F}\mathbf{x}(k) + \mathbf{w}(k)\,, \tag{1}$$

where $\mathbf{x}(k)$ is the state vector of the target at time instant k, $\mathbf{F}$ is the time-invariant state transition matrix and $\mathbf{w}(k)$ a white noise sequence with covariance matrix $\mathbf{Q}(k)$ representing the process noise.

Respectively, the linear measurement models are given by

$$\mathbf{y}_i(k) = \mathbf{H}_i\mathbf{x}(k) + \mathbf{v}_i(k)\,, \tag{2}$$

where $\mathbf{y}_i(k)$ is the observation vector containing the position measurement of the i^{th} sensor, $i = 1, \ldots, N$, $\mathbf{H}_i$ is the corresponding measurement matrix and $\mathbf{v}_i(k)$ a zero-mean, white noise sequence with covariance matrix $\mathbf{R}_i(k)$ representing the measurement noise.

According to these model equations, the *centralized* KF algorithm in its information form with multiple inputs can be described as recursively performing the following two steps to calculate the overall position estimate $\hat{\mathbf{x}}_{\text{KF}}(k|k)$ and error covariance matrix $\mathbf{P}_{\text{KF}}(k|k)$ at time instant k [8]:
1. Prediction

$$\mathbf{P}_{\text{KF}}(k|k-1) = \mathbf{F}\mathbf{P}_{\text{KF}}(k-1|k-1)\mathbf{F}^T + \mathbf{Q}(k-1) \tag{3}$$

$$\hat{\mathbf{x}}_{\text{KF}}(k|k-1) = \mathbf{F}\hat{\mathbf{x}}_{\text{KF}}(k-1|k-1) \tag{4}$$

2. Estimate correction

$$\mathbf{P}_{\text{KF}}^{-1}(k|k) = \mathbf{P}_{\text{KF}}^{-1}(k|k-1) + \sum_{i=1}^{N}\mathbf{H}_i^T\mathbf{R}_i^{-1}(k)\mathbf{H}_i \tag{5}$$

$$\hat{\mathbf{x}}_{\text{KF}}(k|k) = \mathbf{P}_{\text{KF}}(k|k)\Big(\mathbf{P}_{\text{KF}}^{-1}(k|k-1)\hat{\mathbf{x}}_{\text{KF}}(k|k-1) + \sum_{i=1}^{N}\mathbf{H}_i^T\mathbf{R}_i^{-1}(k)\mathbf{y}_i(k)\Big)\,. \tag{6}$$

This is called the information form as the inverse of the covariance matrix $\mathbf{P}^{-1}$ is a measure of the information contained in the corresponding state estimate $\hat{\mathbf{x}}$.

In the *decentralized* KF, the LKFs produce estimates $\hat{\mathbf{x}}_i(k|k)$ based on the information available from a single sensor i using the standard KF equations. At the FC, these estimates are fused together to form the overall state estimate $\hat{\mathbf{x}}_{\text{DKF}}(k|k)$ [4]

$$\mathbf{P}_{\text{DKF}}^{-1}(k|k) = \mathbf{P}_{\text{DKF}}^{-1}(k|k-1) + \sum_{i=1}^{N}\left[\mathbf{P}_i^{-1}(k|k) - \mathbf{P}_i^{-1}(k|k-1)\right] \tag{7}$$

$$\hat{\mathbf{x}}_{\text{DKF}}(k|k) = \mathbf{P}_{\text{DKF}}(k|k)\Big(\mathbf{P}_{\text{DKF}}^{-1}(k|k-1)\hat{\mathbf{x}}_{\text{DKF}}(k|k-1) + \sum_{i=1}^{N}\left[\mathbf{P}_i^{-1}(k|k)\hat{\mathbf{x}}_i(k|k) - \mathbf{P}_i^{-1}(k|k-1)\hat{\mathbf{x}}_i(k|k-1)\right]\Big)\,, \tag{8}$$

where $\mathbf{P}_{\text{DKF}}$ and $\mathbf{P}_i$ are the error covariance matrices of the state estimates $\hat{\mathbf{x}}_{\text{DKF}}$ at the FC and $\hat{\mathbf{x}}_i$ at the LKFs, respectively. Removing the information contained in the predicted estimates $\hat{\mathbf{x}}_i(k|k-1)$ can be considered as decorrelation to render the local corrected estimates $\hat{\mathbf{x}}_i(k|k)$ independent again.

The state estimate $\hat{\mathbf{x}}_{\text{DKF}}(k|k)$ is equivalent to $\hat{\mathbf{x}}_{\text{KF}}(k|k)$ in the centralized KF as the measurements $\mathbf{y}_i(k)$ in Eq. (6) weighted with their inverse covariance matrices are equivalent to the gain in information between the predicted local estimates $\hat{\mathbf{x}}_i(k|k-1)$ and the corrected ones $\hat{\mathbf{x}}_i(k|k)$ in Eq. (8)

$$\mathbf{H}_i^T\mathbf{R}_i^{-1}(k)\mathbf{y}_i(k) = \mathbf{P}_i^{-1}(k|k)\hat{\mathbf{x}}_i(k|k) - \mathbf{P}_i^{-1}(k|k-1)\hat{\mathbf{x}}_i(k|k-1)\,. \tag{9}$$

In many tracking applications measurements are taken in spherical coordinates, e.g. with radar, sonar or optical sensors, whereas the target dynamics are best described in Cartesian ones, e.g. constant velocity or constant acceleration models. Thus, there is a non-linear relationship between the current state $\mathbf{x}(k)$ and the current observations $\mathbf{y}_i(k)$. Therefore, the local KFs need to be replaced by extended KFs (EKFs) and Eq. (2) by the following linearized observation equations [8]

$$\mathbf{y}_i(k) \approx \mathbf{h}(\mathbf{x}_0(k)) + \mathbf{H}(k)(\mathbf{x}(k) - \mathbf{x}_0(k)) + \mathbf{v}_i(k)\,, \tag{10}$$

where the linearized measurement matrix is

$$\mathbf{H}(k) = \left[\frac{\partial\mathbf{h}(\mathbf{x})}{\partial\mathbf{x}}\right]_{\mathbf{x}_0(k)}\,. \tag{11}$$

$\mathbf{h}(\ldots)$ is the non-linear transformation from Cartesian coordinates to spherical ones and $\mathbf{x}_0(k)$ the linearization point.

For EKFs, no proof of optimality exists. On the other hand, it is obvious that taking the most accurate estimate of the current state $\mathbf{x}(k)$ as the linearization point $\mathbf{x}_0(k)$ will lead to the best performance. This estimate is the one at the fusion center $\hat{\mathbf{x}}_{\text{DKF}}(k|k-1)$. If it is fed back to the LKFs, the predicted state estimates of the LKFs in the fusion equations (7, 8) become the same leading to the following fusion equations with feedback [4]

$$\mathbf{P}_{\text{DKF}}^{-1}(k|k) = \sum_{i=1}^{N}\mathbf{P}_i^{-1}(k|k)$$

$$- (N-1)\mathbf{P}^{-1}_{\text{DKF}}(k|k-1) \tag{12}$$

$$\hat{\mathbf{x}}_{\text{DKF}}(k|k) = \mathbf{P}_{\text{DKF}}(k|k)\Big(\sum_{i=1}^{N}\mathbf{P}_i^{-1}(k|k)\hat{\mathbf{x}}_i(k|k) \tag{13}$$

$$- (N-1)\mathbf{P}^{-1}_{\text{DKF}}(k|k-1)\hat{\mathbf{x}}_{\text{DKF}}(k|k-1)\Big)\,.$$

Non-linearities can also be present in the state equation (1). This would require feedback of the global estimate from the FC to the LKFs, too. Thus, resulting in the same fusion equations.

Feedback can also be given in the linear case but no performance improvement at the FC is to be expected from this. According to Eq. (8), it is not the information itself but the gain in information at the LKFs that matters. As stated in Eq. (9), this gain is always equivalent to the information contained in the measurement no matter if feedback is given or not.

3 Communication Constraints

In a distributed fusion network usually many nodes exist, which need to communicate with each other. Therefore, the required bandwidth is likely to be a lot higher compared with a centralized fusion architecture, where all the sensor data is sent to a single processing site. This is especially true if the final estimate shall be obtained at several fusion nodes.

Furthermore, according to Eqs. (7, 8) and Eqs. (12, 13), a communication package in a DKF consists of an estimated state vector along with the inverse of the corresponding error covariance matrix. These are typically of a higher dimension compared with the measurement vector and the measurement error covariance matrix. Therefore, constraints on communication bandwidth are an important issue in DKFs.

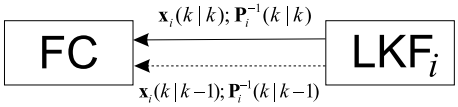

Fig. 2: DKF without feedback

According to Eqs. (7, 8), in a DKF without feedback the FC requires knowledge of $\hat{\mathbf{x}}_i(k|k)$ and $\hat{\mathbf{x}}_i(k|k-1)$ along with $\mathbf{P}_i^{-1}(k|k)$ and $\mathbf{P}_i^{-1}(k|k-1)$ to form the overall estimate. As depicted in Fig. 2, $\hat{\mathbf{x}}_i(k|k)$ and $\mathbf{P}_i^{-1}(k|k)$ necessarily need to be transmitted by the LKFs, but $\hat{\mathbf{x}}_i(k|k-1)$ and $\mathbf{P}_i^{-1}(k|k-1)$ can just as well be calculated at the FC instead. Thus, half of the communication bandwidth can be traded off against a higher computational load at the FC.

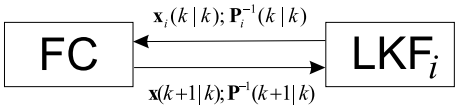

Fig. 3: DKF with feedback

According to Eqs. (12, 13) and as shown in Fig. 3, in a DKF being subject to non-linearities and thus requiring feedback, no such trade-off is possible. The LKFs send $\hat{\mathbf{x}}_i(k|k)$ and $\mathbf{P}_i^{-1}(k|k)$ to the FC after each measurement. The FC in return calculates $\mathbf{P}^{-1}(k|k)$ and $\hat{\mathbf{x}}(k|k)$ predicts them one step ahead and returns them to the LKFs so that the best state estimate can be used as the linearization point. In this case, communication bandwidth can only be saved by sacrificing some performance.

On the other hand, for a large number of sensors, centralized fusion might not even be applicable at all if the central processor cannot handle the large amount of data transmitted by the sensors. In this case, decentralized fusion opens up the possibility to save the necessary bandwidth by letting LKFs communicate with the FC less frequently. Therefore, all predictions by one step need to be replaced with predictions by m steps in Eqs. (7, 8), where $m > 1$ is the factor by which the update rate at the FC is reduced:

$$\mathbf{P}^{-1}_{\text{DKFm}}(k|k) = \mathbf{P}^{-1}_{\text{DKFm}}(k|k-m) + \sum_{i=1}^{N}\left(\mathbf{P}_i^{-1}(k|k) - \mathbf{P}_i^{-1}(k|k-m)\right) \tag{14}$$

$$\begin{aligned}\hat{\mathbf{x}}_{\text{DKFm}}(k|k) = \mathbf{P}_{\text{DKFm}}(k|k)\Big(&\mathbf{P}^{-1}_{\text{DKFm}}(k|k-m)\hat{\mathbf{x}}_{\text{DKFm}}(k|k-m) \\ &+ \sum_{i=1}^{N}\left[\mathbf{P}_i^{-1}(k|k)\hat{\mathbf{x}}_i(k|k)\right. \\ &\left.\left. - \mathbf{P}_i^{-1}(k|k-m)\hat{\mathbf{x}}_i(k|k-m)\right]\right)\,.\end{aligned} \tag{15}$$

Note, however, that the update rate at the LKFs is not affected. The LKFs still run at the sensor observation rate. For dynamic states with process noise, the performance of the fusion process degrades as the information provided by the different sensors becomes correlated due to propagating the same underlying process noise [4, 5, 6].

For less and less frequent communication between the LKFs and the FC, i.e. $m \to \infty$, the information contained in the predicted state estimates becomes less and less reliable. This is represented by the inverses of the corresponding error covariance matrices approaching zero. Thus, no weight is given to these estimates and they can be discarded in Eqs. (7, 8) leading to

$$\mathbf{P}^{-1}_{\text{simple}}(k|k) = \sum_{i=1}^{N}\mathbf{P}_i^{-1}(k|k) \tag{16}$$

$$\hat{\mathbf{x}}_{\text{simple}}(k|k) = \mathbf{P}_{\text{simple}}(k|k)\sum_{i=1}^{N}\mathbf{P}_i^{-1}(k|k)\hat{\mathbf{x}}_i(k|k)\,. \tag{17}$$

This is equivalent to assuming that the local state estimates $\hat{\mathbf{x}}_i(k|k)$ and $\hat{\mathbf{x}}_j(k|k)$ are uncorrelated for all $i \neq j$. Therefore, the estimate $\hat{\mathbf{x}}_{\text{simple}}(k|k)$ can serve as a worst case scenario. More frequent communication necessarily leads to better estimates. Furthermore, $\hat{\mathbf{x}}_{\text{simple}}(k|k)$ can be calculated for every time instant k and not only every m^{th} one as would be the case for $\hat{\mathbf{x}}_{\text{DKFm}}(k|k)$. Thus, less simulation time is needed to achieve statistically significant results.

4 Simulation Results

In this section the amount of performance degradation due to a limited communication bandwidth as presented above shall be estimated by simulations. First, the effects of reducing the feedback rate in a DKF being subject to non-linearities and, second, the effects of reducing the communication rate will be investigated in typical tracking scenarios.

4.1 Reduced Feedback Rate

The following scenario was used to study the impact reducing the frequency of feedback from the FC to the LKFs despite the presence of non-linearities has on the performance. It is an approximation of one of our projects, i.e. a humanoid robot equipped with a microphone array and a stereo-camera observing a human walking around in an office room.

A target moves slowly on a circle with radius $r = 2\,\mathrm{m}$ and at an elevation angle $\phi = \frac{\pi}{4}$ around $N = 2$ sensor systems situated in the origin. During the observation period of $5\,\mathrm{s}$, the target moves from $\theta = -\frac{\pi}{4}$ to $\theta = \frac{\pi}{4}$. Thus, having a centripetal acceleration of $0.20\,\frac{\mathrm{m}}{\mathrm{s}^2}$. The sampling period is $T_s = 0.1\,\mathrm{s}$.

The radius was held fixed to obtain a constant measurement resolution. Transforming measurements with constant resolution in spherical coordinates to Cartesian coordinates leads to a resolution depending on the distance of the target from the sensors. Furthermore, the range resolution of the localization by a microphone array and a stereo-camera is approximately anti-proportional to the range squared, too.

The KFs assumed the target to comply to independent constant velocity models subject to white acceleration noise in the x, y and z-coordinates. As they are identical, only the x-coordinate will be presented in the followings

$$\begin{bmatrix} x(k+1) \\ \dot{x}(k+1) \end{bmatrix} = \begin{bmatrix} 1 & T_s \\ 0 & 1 \end{bmatrix} \begin{bmatrix} x(k) \\ \dot{x}(k) \end{bmatrix} + \mathbf{w}(k)\,, \qquad (18)$$

where

$$\mathbf{w}(k) = \int_0^{T_s} \begin{bmatrix} T_s - t \\ 1 \end{bmatrix} u(kT_s + t)\,dt \qquad (19)$$

and $u(t)$ is a zero-mean continuous random noise sequence with power spectral density N_0, leading to the following process noise covariance matrix

$$\mathbf{Q} = \begin{bmatrix} \frac{1}{3}T_s^3 & \frac{1}{2}T_s^2 \\ \frac{1}{2}T_s^2 & T_s \end{bmatrix} N_0\,. \qquad (20)$$

As the acceleration of an object moving on a circle is deterministic and thus violates the whiteness assumption of the KFs, the power spectral density of the process noise assumed by the DKF was set higher to $N_0 = (0.4\,\frac{\mathrm{m}}{\mathrm{s}^2})^2 \cdot T_s$.

The target was measured in spherical coordinates, i.e. $\mathbf{y}_i(k) = (r, \theta, \phi)^T$. Thus, the measurements can be modeled by Eq. (10), where $i = 1, 2$. The errors in r, θ and ϕ were assumed independent of each other, constant and identical for the different sensors with variances σ_r^2, σ_θ^2 and σ_ϕ^2, resulting measurement error covariance matrices

$$\mathbf{R}_i = \begin{bmatrix} \sigma_r^2 & 0 & 0 \\ 0 & \sigma_\theta^2 & 0 \\ 0 & 0 & \sigma_\phi^2 \end{bmatrix}, \quad i = 1, 2\,. \qquad (21)$$

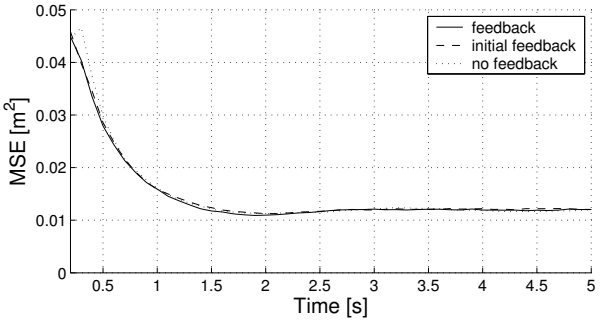

Fig. 4: MSE of the position estimate at the fusion center ($\sigma_r = 0.2\,\mathrm{m}$ and $\sigma_\theta = \sigma_\phi = 4°$)

Figs. 4-6 present the comparison between the Mean Square Error (MSE)

$$\mathrm{MSE} \approx \mathrm{E}\left\{\left(\hat{x}_{\mathrm{DKF}}(k|k) - x(k)\right)^2\right\} \qquad (22)$$

of the position estimate at the fusion center for LKFs receiving feedback after every time step, receiving feedback only once after the initial estimate, and receiving no feedback at all. 5000 Monte Carlo runs were used to average the results.

σ_θ and σ_ϕ were consistently chosen to be $4°$. This is in accordance with the angular resolution of our microphone array. The accuracy of the camera would have been too high to see a noticeable difference between the individual curves. The only difference between the figures is σ_r being increased from $0.2\,\mathrm{m}$ to $0.4\,\mathrm{m}$.

As the initial position estimate at the FC is always only based on the two measurements of the local sensors, all curves start at the same point in each figure. Fig. 4 shows that, even for the relatively moderate value $\sigma_r = 0.2\,\mathrm{m}$, no feedback results in a visible degradation during initialization. Increasing σ_r to $0.3\,\mathrm{m}$, as can be seen in Fig. 5, leads to severe impairments in accuracy, whereas the DKF giving only an initial feedback still follows the curve with feedback after each measurement nicely. Only in Fig. 6, where $\sigma_r = 0.4\,\mathrm{m}$, does this difference become significant, especially during initialization.

These results can be explained by the KFs not taking the additional error due to the linearization into account. During initialization, the position estimate is less accurate. Thus, the linearization error is also bigger during this period leading to the higher sensitivity.

As can be seen in Fig. 7, for $\sigma_r = 0.01\,\mathrm{m}$, the DKF with feedback after each measurement is significantly better than the DKF without feedback again. This is due to the coordinate conversion implicitly used in the EKFs becoming inconsistent for such low values of $\frac{\sigma_r}{r}$ compared with the rather high values of σ_ϕ and σ_θ [9]. According to [10],

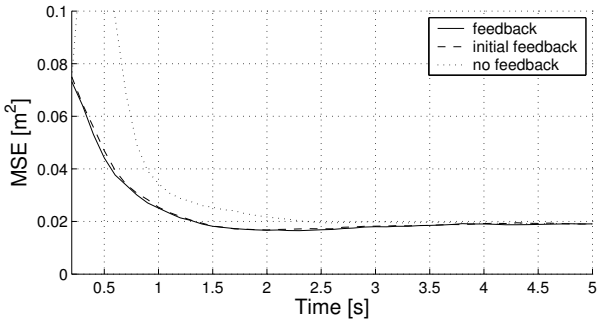

Fig. 5: MSE of the position estimate at the fusion center ($\sigma_r = 0.3\,\mathrm{m}$ and $\sigma_\theta = \sigma_\phi = 4^\circ$)

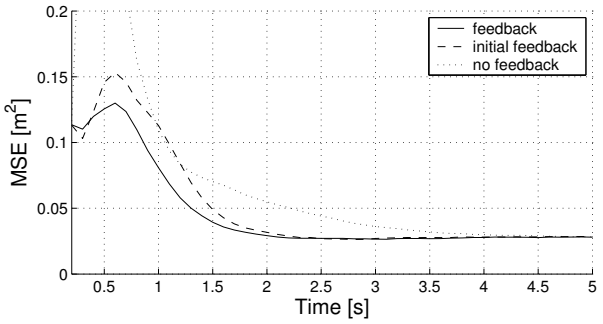

Fig. 6: MSE of the position estimate at the fusion center ($\sigma_r = 0.4\,\mathrm{m}$ and $\sigma_\theta = \sigma_\phi = 4^\circ$)

the validity limit for an EKF performing a conversion from spherical to Cartesian coordinates and an elevation angle $\phi = \frac{\pi}{4}$ is

$$\sigma_r \approx \frac{r\left(\frac{\sigma_\theta^2}{2} + \sigma_\phi^2\right)}{0.48} \approx 0.03\,\mathrm{m}\,. \tag{23}$$

Thus, the LKFs are already at their limits and the extra error strains them even further.

In all figures, the curves with feedback and with initial feedback drop down to a minimum at around $t = 2\,\mathrm{s}$ only to slightly rise afterwards again. This behavior can be explained by the constant acceleration of the target violating the white noise assumption. Thus, the state as predicted by the LKFs is given too much weight compared with the measurement in the steady state. On the other hand, as this rise is rather small, $N_0 = (0.4\,\frac{\mathrm{m}}{\mathrm{s}^2})^2 \cdot T_s$ seems to be a reasonable choice for the process noise.

As the scenarios presented in Figs. 6 and 7 are rarely found for real sensors, it can be concluded that the performance of the state estimate at the fusion center will stay almost unaffected if feedback to the LKFs is given only after initialization. Feedback should still be given from time to time to prevent stability problems at the LKFs under adverse conditions, i.e. if the target is maneuvering or not visible for some sensors etc.

4.2 Reduced Communication Rate

To obtain quantitative measures of the performance degradation due to infrequent communication, again simulations about a target moving at constant velocity, as described by Eq. (18), and tracked by two sensors measuring only its

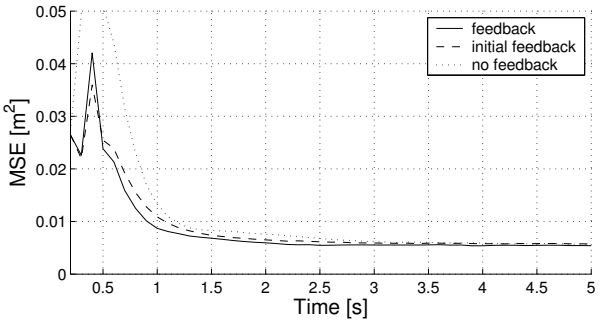

Fig. 7: MSE of the position estimate at the fusion center ($\sigma_r = 0.01\,\mathrm{m}$ and $\sigma_\theta = \sigma_\phi = 4^\circ$)

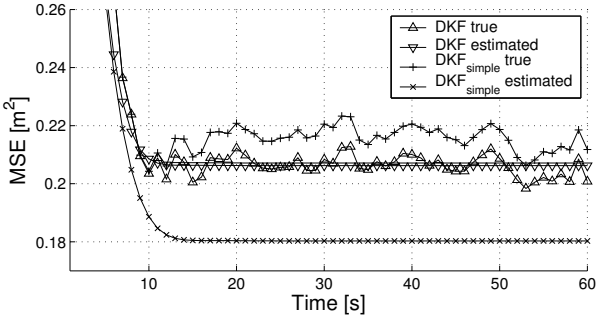

Fig. 8: Comparison between true and estimated MSE of DKF and $\mathrm{DKF_{simple}}$ ($N_0 = 0.01\,\frac{\mathrm{m}^2}{\mathrm{s}^4\mathrm{Hz}}$, $T_s = 1\,\mathrm{s}$, $\sigma_{v,1} = \sigma_{v,2} = 1\,\mathrm{m}$)

position were performed. However, this time the 1D case was examined for simplicity and the measurements were in Cartesian coordinates

$$y_i(k) = [1 \quad 0] \begin{bmatrix} x(k) \\ \dot{x}(k) \end{bmatrix} + v_i(k)\,, \quad i = 1, 2\,, \tag{24}$$

with variances $\sigma_{v,i}^2$. There was no mismatch between the model generating the trajectory of the target and the model assumed by the DKF.

Fig. 8 presents the comparison between the true and estimated MSE of the position component in $\hat{\mathbf{x}}_{\mathrm{DKF}}(k|k)$ and $\hat{\mathbf{x}}_{\mathrm{simple}}(k|k)$ of Eqs. (8, 17) for a typical example where $N_0 = 0.01\,\frac{\mathrm{m}^2}{\mathrm{s}^4\mathrm{Hz}}$, $T_s = 1\,\mathrm{s}$ and $\sigma_{v,1} = \sigma_{v,2} = 1\,\mathrm{m}$. $\sigma_{v,1} = \sigma_{v,2}$ ensures that both sensors have the same impact on the final estimate, which presents the worst case. The "true" MSEs were thereby averaged on 5000 Monte Carlo runs.

It can be seen how the DKF slightly outperforms the $\mathrm{DKF_{simple}}$. Furthermore, the DKF estimates its accuracy correctly whereas the $\mathrm{DKF_{simple}}$, although performing slightly worse, estimates its accuracy even higher than the one of the DKF. These two phenomena will be studied in detail in the followings.

Fig. 9 displays the true MSEs of DKF and $\mathrm{DKF_{simple}}$ averaged over time as a function of the process noise N_0. Again, the sampling period was set to $T_s = 1\,\mathrm{s}$ and the measurement noises to $\sigma_{v,1} = \sigma_{v,2} = 1\,\mathrm{m}$. 200 measurements per simulation and 1000 Monte Carlo runs were used to average the results.

For high values of N_0, both curves approach the vari-

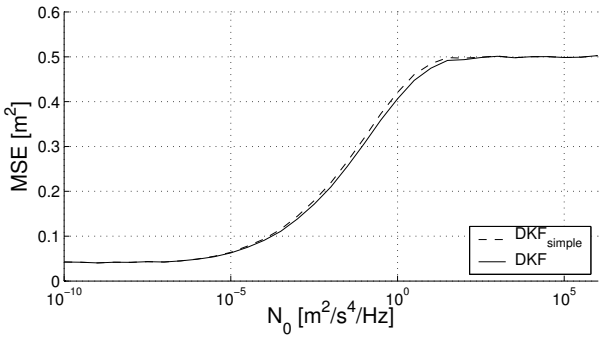

Fig. 9: Comparison between $\text{MSE}_{\text{simple}}$ and MSE_{DKF} as a function of the process noise N_0 ($T_s = 1\,\text{s}$, $\sigma_{v,1} = \sigma_{v,2} = 1\,\text{m}$)

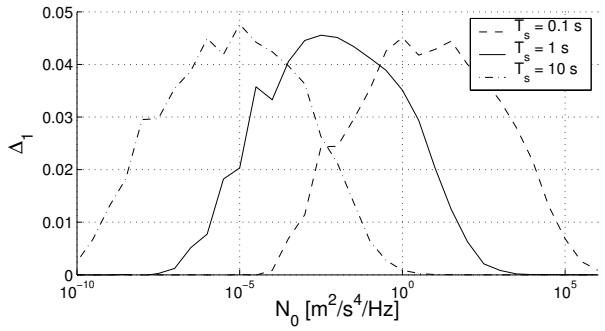

Fig. 10: Relative difference between $\text{MSE}_{\text{simple}}$ and MSE_{DKF} as a function of the process noise N_0 ($\sigma_{v,1} = \sigma_{v,2} = 1\,\text{m}$)

ance of the combined measurements $\sigma^2_{v,\text{comb}} = \frac{\sigma^2_{v,1}\sigma^2_{v,2}}{\sigma^2_{v,1}+\sigma^2_{v,2}} = 0.5\,\text{m}^2$. For low values of N_0, they should approach zero as KFs are able to estimate the position arbitrarily precisely if no process noise is present and if a sufficient number of observations is available. Due to calculating the MSEs only on 200 samples including the initialization phase, this is not the case here.

It can be seen that the difference between the two curves approaches zero for very small and for very large values of N_0. This can be illustrated as follows. For very small values of N_0, the noise term in the state equation (18) approaches zero. Thus, there is practically no process noise whose propagation could be responsible for the statistically dependence of the information of the two LKFs.

On the other hand, very large values of N_0 mean an unreliable prediction. Thus, the predicted states $\hat{\mathbf{x}}_i(k|k-1)$, although correlated, carry almost no information about the current state $\mathbf{x}(k)$. Accordingly, they are given almost no weight compared with the measurements $\mathbf{y}_i(k)$ in calculating $\hat{\mathbf{x}}_i(k|k)$ in the LKFs. Note that the Kalman filters are of little use in this case.

Fig. 10 shows the relative difference

$$\Delta_1 = \frac{\text{MSE}_{\text{simple}} - \text{MSE}_{\text{DKF}}}{\text{MSE}_{\text{DKF}}} \tag{25}$$

between these two curves in Fig. 9 and for additional values of the sampling period T_s. In Fig. 11, the corresponding results for varying measurement noises $\sigma_{v,1}$ and $\sigma_{v,2}$ are

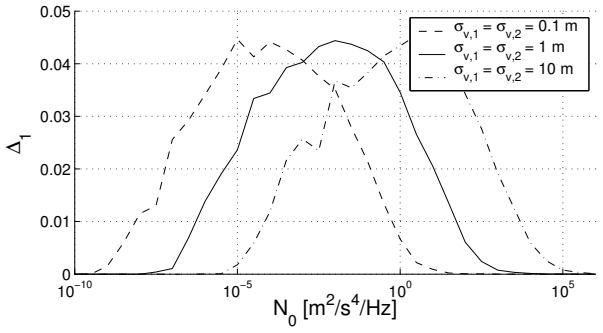

Fig. 11: Relative difference between $\text{MSE}_{\text{simple}}$ and MSE_{DKF} as a function of the process noise N_0 ($T_s = 1\,\text{s}$)

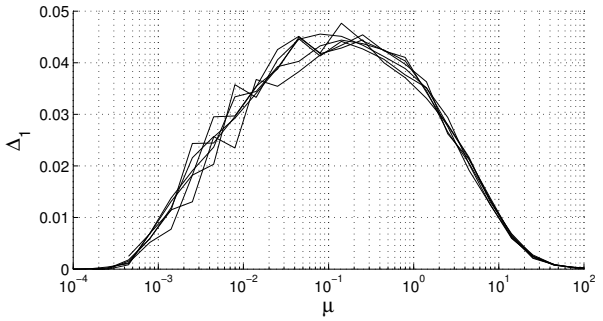

Fig. 12: Relative difference between $\text{MSE}_{\text{simple}}$ and MSE_{DKF} as a function of the target maneuvering index μ

presented.

In both figures changing the parameter merely results in a shift of the corresponding curve. Its shape is not affected. If T_s is increased by a factor of 10, N_0 needs to be decreased by a factor of 1000 to obtain the same results. On the other hand, if $\sigma_{v,1}$ and $\sigma_{v,2}$ are increased by a factor of 10, N_0 needs to be increased by a factor of 100.

As indicated in Eq. (20), $\frac{1}{3}N_0T_s^3$ is equivalent to the variance of the position estimate due to the process noise $\mathbf{Q}^{11}$. Thus, the ratio between $\mathbf{Q}^{11}$ and $\sigma^2_{v,\text{comb}}$ needs to be constant to obtain the same result. This ratio indicates how much weight is given to the predicted estimate and the measurements during the fusion process, respectively.

Alternatively, the target maneuvering index [11]

$$\mu = \sqrt{\frac{N_0T_s^3}{\sigma^2_{v,\text{comb}}}} \tag{26}$$

can be chosen as the function variable, too. The corresponding results are plotted in Fig. 12. The invariance of the curves with respect to μ can be seen clearly.

The maximum of the curves in Fig. 12 is rather broad. It ranges approximately from $\mu = 5 \cdot 10^{-3}$ to $\mu = 5$. Thus, many typical scenarios for applying Kalman filters fall within this range. In our scenario the typical acceleration of the target, i.e. a human, is approximately $0.3\,\frac{\text{m}}{\text{s}^2}$, the measurement accuracy $0.1\,\text{m}$ and the sampling period $0.1\,\text{s}$. This leads to a target maneuvering index μ of around 0.03, which also lies within the maximum.

Note that in Fig. 12 the variance in estimating the difference becomes bigger for smaller values of μ. This is due

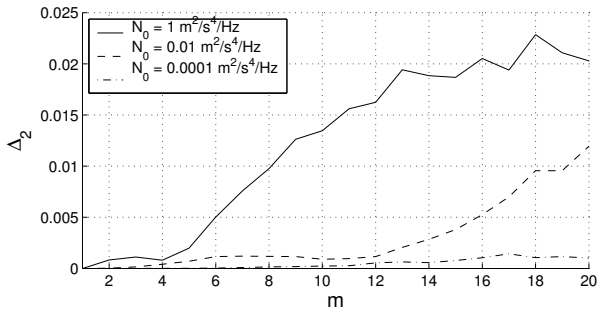

Fig. 13: Relative difference between MSE_{DKFm} and MSE_{DKF} as a function of the the update rate m ($T_s = 1\,\text{s}$, $\sigma_{v,1} = \sigma_{v,2} = 1\,\text{m}$)

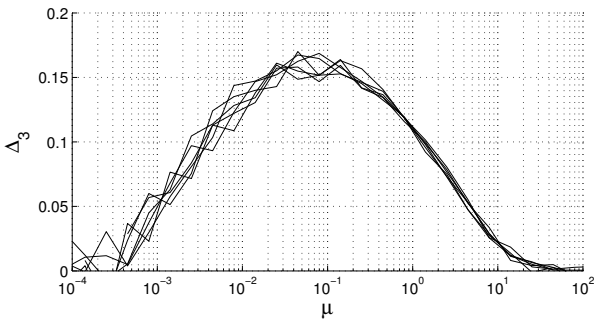

Fig. 14: Relative difference between true and estimated MSE of $\text{DKF}_{\text{simple}}$ as a function of the target maneuvering index μ

to the errors of the state estimate of a KF becoming more correlated in time for such values of μ. Thus, the effective number of samples is reduced on which the average in Eq. (25) is performed.

It remains to be examined how quickly the maximal degradation of 4 to $5\,\%$ as indicated in Figs. 10-12 is reached. To this end, Fig. 13 shows the relative difference

$$\Delta_2 = \frac{\text{MSE}_{\text{DKFm}} - \text{MSE}_{\text{DKF}}}{\text{MSE}_{\text{DKF}}} \tag{27}$$

between the MSE of the position component in $\hat{\mathbf{x}}_{\text{DKFm}}(k|k)$ and $\hat{\mathbf{x}}_{\text{DKF}}(k|k)$ of Eqs. (15, 8) as a function of the update rate m for three interesting values of N_0. Again, the sampling period was set to $T_s = 1\,\text{s}$ and the measurement noises to $\sigma_{v,1} = \sigma_{v,2} = 1\,\text{m}$. This time 10000 Monte Carlo runs were performed on simulations with 200 measurements.

It can be seen that the maximum difference is reached more slowly for smaller power spectral densities of the process noise N_0. This can be explained with the state vector $\mathbf{x}(k)$ changing only slowly in these scenarios. Therefore, the estimate of the term correcting for the correlation between $\hat{\mathbf{x}}_1(k|k)$ and $\hat{\mathbf{x}}_2(k|k)$ of the DKFm

$$\begin{aligned}\mathbf{X}_{\text{DKFm}} = {} & \mathbf{P}^{-1}_{\text{DKFm}}(k|k-m)\hat{\mathbf{x}}_{\text{DKFm}}(k|k-m) \\ & - \mathbf{P}_1^{-1}(k|k-m)\hat{\mathbf{x}}_1(k|k-m) \\ & - \mathbf{P}_2^{-1}(k|k-m)\hat{\mathbf{x}}_2(k|k-m)\end{aligned} \tag{28}$$

stays longer an accurate estimate of the correct term

$$\begin{aligned}\mathbf{X}_{\text{DKF}} = {} & \mathbf{P}^{-1}_{\text{DKF}}(k|k-1)\hat{\mathbf{x}}_{\text{DKF}}(k|k-1) \\ & - \mathbf{P}_1^{-1}(k|k-1)\hat{\mathbf{x}}_1(k|k-1) \\ & - \mathbf{P}_2^{-1}(k|k-1)\hat{\mathbf{x}}_2(k|k-1)\,.\end{aligned} \tag{29}$$

As a result, it can be concluded that for all simulated scenarios the communication rate between the LKFs and the FC can be reduced by at least a factor of 8 without introducing an additional error of more than $1\,\%$. Furthermore, for sensors producing measurements at high frequencies, i.e. scenarios where a reduction in communication rate is likely to be desirable, the error due to infrequent communication is typically even smaller due to the short sampling period T_s and, thus, the small target maneuvering index μ.

KFs do not only produce state estimates $\hat{\mathbf{x}}$ but also calculate an accuracy of these estimates in form of the error covariance matrix $\mathbf{P}$. As stated earlier, the DKF estimates its accuracy correctly whereas the $\text{DKF}_{\text{simple}}$, although performing slightly worse, estimates its accuracy even higher than the one of the DKF.

Fig. 14 shows this difference Δ_3 between the true and estimated MSE of the $\text{DKF}_{\text{simple}}$ as a function of the target maneuvering index μ. The "true" MSEs were thereby averaged on 5000 Monte Carlo runs. The shape of these curves is very similar to the ones in Fig. 12 for the difference between the true MSE of the $\text{DKF}_{\text{simple}}$ and the DKF. The maximum is only higher at around $16\,\%$. This overestimation presents a significant drawback of the $\text{DKF}_{\text{simple}}$ as the correct prediction of the accuracy is a big advantage when designing a system.

5 Asynchronous Measurements

Eqs. (7, 8) do not only require the LKFs to communicate with the FC after each measurement. Synchronous measurements are implicitly assumed, too. On the other hand, the results of the previous section have shown that the error introduced due to infrequent communication is likely to be almost negligible. Thus, a very simple alternative seems viable: The LKFs all run at their own observation rate communicating with the FC only at predetermined times as defined by the sampling period T_{FC}.

To this end, the LKFs must be able to determine predicted state estimates $\hat{\mathbf{x}}_i(t_1|t_2)$ along with the corresponding error covariance matrices $\mathbf{P}_i^{-1}(t_1|t_2)$ for arbitrary times t_1 and t_2 corresponding to multiples of the sampling period of the FC and the LKF, respectively. This requires the matrices $\mathbf{F}$ and $\mathbf{Q}$ to be set up for arbitrary time intervals. As far as $\mathbf{F}$ is concerned and as (1) is normally derived from a continuous model, this task is likely to be trivial.

As far as $\mathbf{Q}$ is concerned, the discrete white noise sequence $\mathbf{w}(k)$ in Eq. (1) has to be assumed to be generated from a continuous white noise sequence $u(t)$ as shown for a constant velocity model in Eq. (19). The frequently found assumption of $\mathbf{w}(k)$ being produced by a discrete white noise sequence $u(k)$

$$\mathbf{w}_2(k) = \begin{bmatrix} \frac{1}{2}T_s^2 \\ T_s \end{bmatrix} u(k) \tag{30}$$

with variance σ_u^2, and thus leading to the following process

noise covariance matrix

$$\mathbf{Q}_2 = \begin{bmatrix} \frac{1}{4}T_s^4 & \frac{1}{2}T_s^3 \\ \frac{1}{2}T_s^3 & T_s^2 \end{bmatrix} \sigma_u^2 \,, \tag{31}$$

cannot be made. This model implicitly assumes $u(k)$ to be constant between two samples. If this assumption is true for a given sampling period T_s, it cannot be true for any other T_s [11].

However, the difference between $\mathbf{w}(k)$ and $\mathbf{w}_2(k)$ is rather small if the changes in the target velocity between two sampling points shall be the same, i.e.

$$\sqrt{\mathbf{Q}^{22}} = \sqrt{N_0 T_s} \stackrel{!}{=} \sigma_u T_s = \sqrt{\mathbf{Q}_2^{22}} \,. \tag{32}$$

This is equivalent to the discrete white noise sequence $u(k)$ being a sampled version of the continuous white noise sequence $u(t)$, which has been limited to a bandwidth B as defined by the sampling period T_s

$$\sigma_u^2 = \frac{N_0}{T_s} = N_0 B \,. \tag{33}$$

Under this assumption

$$\mathbf{Q}_2 \approx \mathbf{Q} \,. \tag{34}$$

However, the difference increases for higher orders of the system model.

Communication delays can be incorporated in the above approach as well. If they are known beforehand, they can easily be taken into account when calculating $\hat{\mathbf{x}}_i(t_1|t_2)$ and $\mathbf{P}_i^{-1}(t_1|t_2)$.

6 Conclusions

This paper focuses on the impact, which infrequent communication has on the performance of a DKF. As a result it can be concluded that for all simulated scenarios the communication rate between the LKFs and the FC can be reduced significantly in both directions.

If the measurements are in spherical coordinates whereas the state vector is in Cartesian ones and, thus, the LKFs require feedback from the FC for optimal performance, this feedback can be limited to the initialization phase and adverse conditions without introducing a significant additional error. Furthermore, the LKFs can also reduce the rate at which they communicate with the FC by at least a factor of 8 without introducing an additional error of more than $1\,\%$. On the other hand, the DKF significantly overestimates its accuracy if the correlation between the inputs is not taken into account. This is a significant drawback when designing a tracking system.

Finally, based on these findings concerning the possible reduction in communication rate, a simple approach to deal with asynchronous measurements and communication delays between the LKFs and the FC was presented.

7 Acknowledgments

This work is part of the Sonderforschungsbereich (SFB) No. 588 *"Humanoide Roboter - Lernende und kooperierende multimodale Roboter"* at the University of Karlsruhe. The SFB is supported by the Deutsche Forschungsgemeinschaft (DFG).

References

[1] K.C. Chang, X. Yin, and R. K. Saha. Evaluating a linear predictive algorithm for bandwidth conservation. *IEEE Transactions on Aerospace and Electronic Systems*, 36(4):1407–1414, 2000.

[2] B.S. Rao and H.F. Durrant-Whyte. Fully decentralised algorithm for multisensor Kalman filtering. *IEE Proceedings-Control Theory and Applications*, 138(5):413–420, Sep 1991.

[3] N. Strobel, S. Spors, and R. Rabenstein. Joint Audio-Video Object Localization and Tracking. *IEEE Signal Processing Magazine*, 18(1):22–31, 2001.

[4] M.E. Liggins, C.-Y. Chong, I. Kadar, M.G. Alford, V. Vannicola, and S. Thomopoulos. Distributed Fusion Architectures and Algorithms for Target Tracking. *Proceedings of the IEEE*, 85(1):95–107, Jan 1997.

[5] K.C. Chang, R.K. Saha, and Y. Bar-Shalom. On Optimal Track-to-Track Fusion. *IEEE Transactions on Aerospace and Electronic Systems*, 33(4):1271–1276, Oct 1997.

[6] O.E. Drummond. On track and tracklet fusion filtering. In *Signal and Data Processing of Small Targets 2002, Proc. SPIE*, volume 4728, pages 176–194, 2002.

[7] A.T. Alouani and T.R. Rice. On optimal asynchronous track fusion. In *First Australian Data Fusion Symposium*, pages 147–152, Nov 1996.

[8] R.G. Brown. *Introduction to Radom Signal Analysis and Kalman Filtering*. New York: John Wiley & Sons, 1983.

[9] P. Suchomski. Explicit Expressions for Debiased Statistics of 3D Converted Mmeasurements. *IEEE Transactions on Aerospace and Electronic Systems*, 35(1):368–370, Jan 1999.

[10] M.S. Schlosser and K. Kroschel. Limits in Tracking with Extended Kalman Filters. submitted to IEEE Transactions on Aerospace and Electronic Systems, 2003.

[11] Y. Bar-Shalom and T. Fortmann. *Tracking and Data Association*. New York: Academic Press, 1988.